(21) Graessley, W. W. *Polymer* **1980**, *21*, 258.
(22) Edwards, S. F. Reported at the U.S.-France Seminar on Polymer Solutions and Melts, Lac Du Flambeau, WI, 1980.
(23) Amis, E. J.; Han, C. C. *Polymer* **1982**, *23*, 1403.
(24) Reference 5, p 225.
(25) Schmidt, M.; Burchard, W. *Macromolecules* **1981**, *14*, 210.
(26) Amis, E. J.; Janmey, P. A.; Ferry, J. D.; Yu, H. *Polym. Bull.* **1981**, *6*, 13.

Structural Characterization of an Ethylene–Tetrafluoroethylene Alternating Copolymer by Polarized Raman Scattering

Karen Zabel,† N. E. Schlotter, and John F. Rabolt*

IBM Research Laboratory, San Jose, California 95193. *Received May 15, 1982*

ABSTRACT: The anisotropic scattering properties of a uniaxially oriented filament of an ethylene–tetrafluoroethylene (E–TFE) alternating copolymer have been investigated in order to determine the molecular conformation in ordered crystalline regions. Both a trans-planar and a 3/2-helical structure have been shown to be energetically possible in an isolated molecule and in this study the group theoretical analyses for these structures are presented. Comparison of these results with polarized Raman measurements indicates that the copolymer backbone crystallizes in predominantly a planar-zigzag structure. Observation of the low-frequency Raman-active longitudinal acoustical mode (LAM) and the correlation of its frequency position with the crystalline stem length obtained from SAXS and crystallinity measurements strongly support the trans-planar structure.

Introduction

Studies of molecular orientation in polymers can be useful in determining the conformational, crystal, and morphological structure[1-7] as well as in determining correlations between these microscopic structures and macroscopic properties. In highly oriented polymers the structural symmetry of the chain and crystal will give rise to spectroscopic selection rules that govern spectral activity in both the infrared and Raman spectrum. When several conformational or crystal structures have been proposed by other methods it is often possible to identify the correct one by using the results obtained from vibrational spectroscopy on a highly oriented sample.

Alternating copolymers of E–TFE, synthesized by radical copolymerization, were reported by Modena et al.[8] to exhibit high alternation. Subsequent studies by X-ray photoelectron spectroscopy,[9] NMR,[10] and ESCA[11] have since substantiated these results. This copolymer exhibits a high melting point and thermal stability[12] but is also interesting from a molecular point of view since the chemical repeat unit, $-CH_2CH_2CF_2CF_2-$, is a model of a head-to-head structural defect in poly(vinylidene fluoride) (PVF_2), which is known to contain 5–10% of such defect linkages.

An early investigation[13] of the crystal and molecular structure by wide-angle X-ray scattering (WAXS) indicated that the conformation was most likely planar zigzag, possibly with slight twisting, while the chains packed into either an orthorhombic or monoclinic lattice. Conformational energy calculations by Farmer and Lando[14] found that if an isolated chain was alone considered, then the minimum-energy conformation would, in fact, be a 3/2 helix rather than a trans-planar structure. Interestingly, when these chains were packed into a crystal lattice, the planar-zigzag structure became the energetically favorable conformation. Their results also indicated that five different crystal packing schemes were possible and approximately equal in energy with one being similar to that suggested by Wilson and Starkweather[13] in their original X-ray studies.

In this work the anisotropic scattering properties of a highly oriented filament of an E–TFE alternating copolymer have been determined and used together with group theoretical analyses to identify the chain conformation in the solid state. An intense low-frequency Raman band assignable to a longitudinal acoustical mode (LAM) has been observed and its polarized scattering used in conjunction with its band position as convincing evidence for a planar-zigzag conformation.

Experimental Section

The alternating copolymer of ethylene and tetrafluoroethylene used in this study was a commercial DuPont material, Tefzel 280. It was extruded and then highly drawn into an oriented transparent monofilament (by the Albany Monofilament Co.) with a diameter of 0.008 in. All Raman spectra were taken on monofilament samples as received.

The DSC melting point measurements were determined using a DuPont Model 990 thermal analyzer.

The infrared spectra of the E–TFE copolymer was obtained with an IBM 9198 vacuum Fourier transform interferometer with 2-cm^{-1} resolution. The thin-film samples for the infrared transmission studies were prepared by pressing the melted copolymer between the heated plates of a Carver press. An IR polarizer was employed to ensure that the films produced by this technique were isotropic.

Raman spectra were recorded with a Jobin-Yvon Ramanor HG-2S double monochromator using the 5145-Å line of a Spectra Physics 165-04 argon ion laser equipped with a temperature-stabilized etalon. To collect the polarized Raman spectra away from the Rayleigh line the input laser beam was passed through a 5145-Å narrow-band filter (less than 50-cm^{-1} band-pass), the polarization was selected via a polarization rotator, and the beam was passed through a Glan-Thompson polarizing prism to remove any components whose polarization may have been scrambled by passage through optical elements and finally focused on the sample. The scattered Raman signal was collected by a lens matched to the monochromator, passed through an oriented polarization analyzer, and scrambled to eliminate intensity differences due to the anisotropic diffraction properties of holographic gratings.

A conventional way to record Raman spectra of oriented filaments is schematically illustrated in Figure 1. The filament is clamped in a vertical position with the incoming laser polarization

†Summer Research Student (1981); present address: Department of Chemistry, San Francisco State University, San Francisco, CA 94132.

0024-9297/83/2216-0446$01.50/0

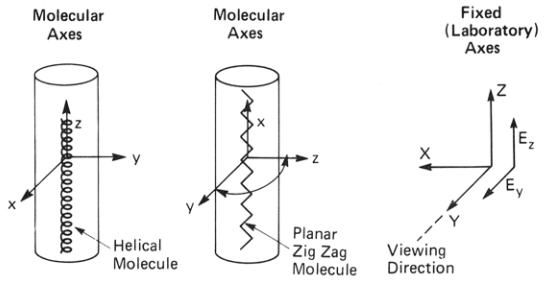

Figure 1. Orientational relationship between molecular and laboratory axes used in recording Raman spectra (geometry 1).

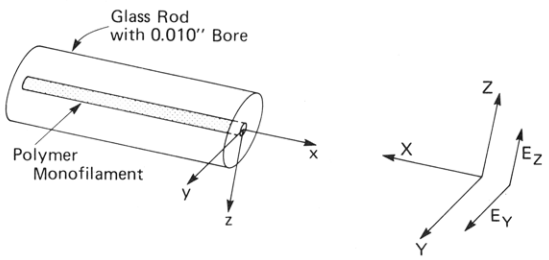

Figure 2. Scattering geometry and relationship between molecular and laboratory axes for recording of Raman spectra (geometry 2) of uniaxially oriented E–TFE through end of filament.

adjusted to lie either parallel or perpendicular to the macroscopic filament axis. A second nonconventional scattering geometry, shown in Figure 2, was used in order to assist in making band assignments to specific symmetry species. In this case, a piece of E–TFE filament (0.008-in. diameter), which had been cut with a new razor blade, was placed inside a glass rod (outside diameter = 0.22 in.) that had an inner bore diameter of 0.010 in. After the rod was mounted so that it was parallel to the surface of the table, the incident laser (after tight focusing by a 50-mm achromat lens) could be brought through the end of the filament. Scattered light from the first 2–3 mm (to minimize any polarization scrambling of the filament) was collected at 90° through the side of the glass rod and focused onto the entrance slit of the double monochromator. As will be shown in a later section, this changes the contribution of the various derived polarizability tensor elements to the scattering intensity, and in conjunction with other measurements using the standard geometry depicted in Figure 1, it allows the assignment of each band to a specific symmetry species.

Measurements of the low-frequency longitudinal acoustical mode (LAM) required several additions to the collection optics. An optical cell containing I_2 vapor maintained at 80 °C was placed between the collection lens and the monochromator. Passing the collected scattered light from the sample through this filter causes attenuation of the elastically scattered Rayleigh component by as much as 6 orders of magnitude while the intensity of the Raman scattering will be decreased by only 50% due to absorption by the I_2 in the cell.[15] This technique in conjunction with the superior stray light rejection afforded by the four-slit configuration of the Ramanor (containing holographic gratings) allows spectra to be recorded within 3 cm^{-1} of the exciting line. All the data were collected and processed with a Nicolet 1180 data system. Spectra with sufficient S/N were obtained at 2-cm^{-1} band-pass by the coaddition of 35 scans. Correction of the LAM band intensity for I_2 absorption, stray light, temperature, and frequency was made according to Snyder and Scherer.[16]

Results and Discussion

A. Evidence for High Alternation. From the exceptionally small product of the reactivity ratios[17] for the ethylene (E) and tetrafluoroethylene (TFE) monomers it would be expected that E–TFE copolymers, polymerized at low temperatures, would be highly alternating. This was verified experimentally by Modena et al.[8] for a series of copolymers polymerized from different mole percentages of E and TFE starting monomers. Additional characterization of E–TFE copolymers by NMR[10] and X-ray photoelectron spectroscopies[9] indicates that alternations of 90% are common and in some cases extremely high alternation (>95%) has been observed.

The commercial copolymer used in this study was melt pressed into an isotropic thin film suitable for IR investigation. A weak shoulder observed at 1474 cm^{-1} is indicative of a small amount of $(-CH_2CH_2-)_n$ groups with $n > 2$. There is also a small amount of $(-CH_2CH_2-)_n$ sequences with $n = 2$ as evidenced[8] by a very weak band at 733 cm^{-1}. Since the intensity of the bands in an absorption spectrum is directly proportional to the concentration of the molecular species, these results suggest that the number of chemical defects is small (<8–10%). Additional evidence is provided by differential scanning calorimetry (DSC), which yielded a single-peak melting point at 269 °C. Although the crystalline melting point can vary slightly depending on thermal processing history, the observed value is consistent with a 50/50 mol % copolymer containing high alternation.[8,12]

Raman measurements on the as-received E–TFE showed no evidence in either the 1400–1450-cm^{-1} $-CH_2-$ bending region or the 1050–1150-cm^{-1} –CC– stretching region for any significant $-CH_2-$ block formation.

Thus the above results taken collectively suggest that the sample used in this study was a highly alternating copolymer of E and TFE similar to that used in earlier studies.[8-11]

B. Evidence for Orientation. WAXS and SAXS measurements were obtained in order to determine the extent of orientation in the E–TFE filament. The WAXS photographs were obtained in transmission and were used only as a qualitative measure of orientation. The three observed d spacings at 4.60, 5.09, and 11.8 Å were highly arced, indicative of a high degree of orientation, which would be expected for an extruded filament subjected to a high draw ratio. This is in contrast to that characteristic of drawn films, which has been reported[18] in the literature.

The SAXS measurements of the E–TFE filament yielded a four-point pattern indicative of lamellar tilt with respect to the macroscopic filament axis.[19] The angle of tilt was determined to be 36–38°. However, the anisotropic scattering properties of the Raman-active LAM indicated that, within experimental error, the chain stems are parallel to the filament axis and hence are inclined with respect to the lamella surface.

C. Polarized Raman Measurements. The scattering geometry (90°) used to obtain polarized Raman measurements, and on which the ensuing group theoretical analysis will be based, is shown in Figure 1. In the laboratory frame of reference the incident laser beam propagates along the X axis while the scattered light is viewed along the Y axis. The incident light can be polarized along either the Z or Y direction while the analyzer can be placed parallel to either the X or Z axis. The designation for each Raman spectrum describing the scattering geometry, incident polarization, and position of analyzer is due to Porto[20] and is used to label the spectra in Figure 3. The scattering notation is of the form $A(BC)D$, where A and D are the propagation directions of the incident (A) and scattered (D) radiation, while B and C refer to the direction of polarization of the incident (B) and analyzed (C) radiation, respectively. Thus in the top spectrum of Figure 3 the incident beam propagates along the laboratory X axis with polarization parallel to Z. The scattered radiation was viewed along Y through a polarizer aligned parallel to the laboratory Z axis.

As can be seen in Figures 3 and 4 the anisotropic scattering properties of the filament are evident. This par-

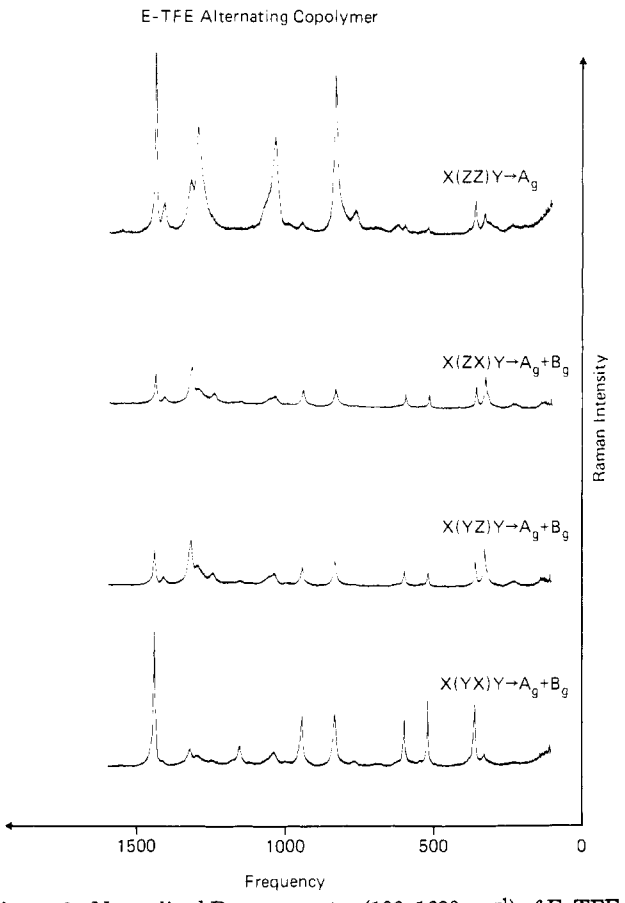

Figure 3. Normalized Raman spectra (100–1600 cm^{-1}) of E–TFE copolymer filament obtained from four combinations of polarizer and analyzer positions in a 90° scattering geometry (geometry 1).

ticular set of polarized Raman experiments was designed to select out modes belonging to each of the Raman-active symmetry species through knowledge of the chain orientation with respect to the filament axis, the factor group symmetry, and the Raman scattering activities. In this case, two conformational models were considered: a planar zigzag and a 3/2 helix. As described previously the former has been found[14] to be the most energetically favorable in a crystal lattice while the latter is the minimum-energy conformation for an isolated molecule. The Raman scattering activities have been worked out by Snyder[21] for partially oriented systems in which the unique axis of the point group (by virtue of its being an axis of rotation or perpendicular to a reflection plane) lies parallel to the orientation direction. These scattering activities were tabulated in terms of derived polarizability elements for the usual point groups in both 90° and 180° scattering. Although helical symmetry groups such as $C(4\pi/3)$ were not specifically considered, use of his tables can be made by correlating Raman-active symmetry species of the helical group to those of the point groups considered. In the helical example used in this analysis, the scattering activities of the Raman-active symmetry species of $C(4\pi/3)$ are identical with those of the point group C_3.

In the planar conformation for E–TFE, the factor group of the line group is isomorphic with the C_{2h} point group. Therefore, the unique axis (C_2) of the point group is perpendicular to the plane of the molecule and therefore perpendicular to the chain axis or orientation direction. This means that the relationship between the orientation direction of the sample and the unique axis of the point group is different from the cases treated by Snyder.[21] New

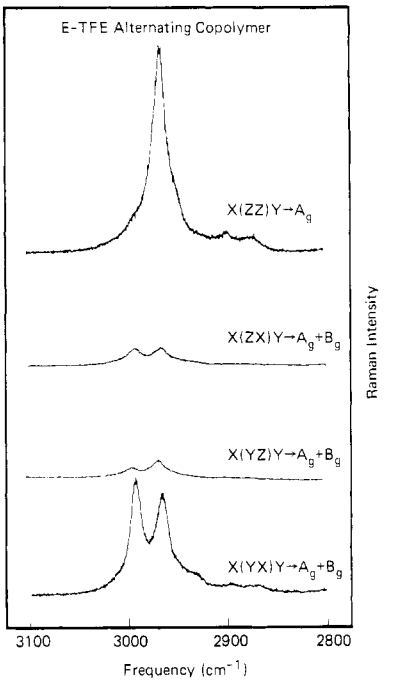

Figure 4. Raman spectra (2800–3100 cm^{-1}) in the CH stretching region of an E–TFE uniaxially oriented filament obtained as a function of polarizer and analyzer position. Weak bands at 2870 and 2897 cm^{-1} result from $(CH_2)_n$ ($n > 2$) defects (geometry 1).

orientation averages must be calculated taking into account the new relationship between the sample orientation direction and the unique axis of the point group. In this case the Raman scattering activities have not been worked out although Boerio and Bailey[3] have determined them for the special case of poly(ethylene terephthalate) fibers. For our uniaxially oriented filament in the scattering geometry (90°) illustrated in Figure 1, the Raman scattering activities in terms of the principal axes of polarizability of the molecule were determined. The chain axis is parallel to the x axis of the molecule while the unique axis (by virtue of the C_2 axis) lies parallel to the molecular z axis. Since the sample is uniaxially oriented, the y and z axes can have all possible orientations in the laboratory XY plane. Therefore in order to determine the derived polarizability tensor elements in the laboratory axes (XYZ), one must orientationally average the y and z component elements in the laboratory XY plane. Details of the calculations for the cases not considered by Snyder[21] will be given elsewhere[22] but the quantity required is the transformation matrix, Φ, relating the laboratory axes to the molecular axes. In this case

$$\Phi = \begin{bmatrix} 0 & -\sin\theta & -\cos\theta \\ 0 & \cos\theta & -\sin\theta \\ 1 & 0 & 0 \end{bmatrix} \quad (1)$$

where θ is the angle between the y and Y axes. The derived polarizabilities, $\alpha_{FF'}$, in the laboratory axes can then be determined by using the expression

$$\alpha_{FF'}{}^2 = \langle (\sum_{gg'} \Phi_{Fg}\Phi_{F'g'}\alpha_{gg'})^2 \rangle \quad (2)$$

where F and F' are the incident and scattered polarization direction, respectively, whereas the $\alpha_{gg'}$ are the derived polarizability tensor elements in the molecular coordinate system. For planar E–TFE, the factor group C_{2h} then determines the derived polarizability tensor elements contributing to the Raman scattering activities.

Table I
Raman Scattering Activities for Planar and Helical Structures of the E-TFE Copolymer

polarization expt	planar zigzag (C_{2h})		3/2 helix (C_3)	
	A_g	B_g	A	E
$X(ZZ)Y$	α_{xx}	0	α_{zz}	0
$X(ZX)Y$	α_{xy}	α_{xz}	0	α_{yz}, α_{zx}
$X(YZ)Y$	α_{xy}	α_{xz}	0	α_{yz}, α_{zx}
$X(YX)Y$	α_{yy}, α_{zz}	α_{zy}	0	α_{xx}, α_{yy}, α_{xy}

Table II
Symmetry Assignment of the Polarized Raman Bands

symmetry	obsd freq, cm^{-1}	symmetry	obsd freq, cm^{-1}
A_g	2966	B_g	2992
	1441		1321
	1299		1247
	1037		1153
	945		945
	(tentative)		328
	835		132
	600		
	520		
	360		
	234		

In Table I the results for both the 3/2-helical (C_3) and the planar-zigzag (C_{2h}) conformations are compared. For each of the polarization experiments the symmetry species that would be Raman active, and therefore observed in the spectrum, are shown for the two conformational models considered. Several important conclusions can be drawn from this table, which when used in conjunction with the observed spectra can be useful in identifying the backbone structure.

In both the $X(ZX)Y$ and $X(YZ)Y$ experiments (Table I) the observed Raman spectra are predicted to be identical and thus will not provide a means of differentiation between the two possible chain conformations. This is, in fact, observed by reference to the similarly labeled spectra of Figures 3 and 4. In contrast, the $X(ZZ)Y$ measurement will in both models select out only the totally symmetric symmetry species (A_g and A) and when taken in conjunction with the results of the $X(YX)Y$ experiment a discernible difference becomes apparent. Whereas for a helical backbone these two measurements would predict the absence of the totally symmetric species in the $X(YX)Y$ spectrum, the predictions for a planar structure indicate the appearance of bands assignable to both A_g and B_g symmetry species in the $X(YX)Y$ experiment. A comparison of the upper and lower spectra of Figure 4 indicates dramatically that this is in fact the case. For example, the $X(ZZ)Y$ spectrum contains only the 2966-cm^{-1} CH stretching mode while the observed spectrum in the $X(YX)Y$ geometry clearly shows the presence of the 2966-cm^{-1} band plus an additional CH stretching component at 2992 cm^{-1} belonging to the B_g symmetry species. Additional evidence is provided by comparison of the corresponding spectra in Figure 3. For a 3/2 helix the two measurements should yield totally different Raman spectra since either the A or E symmetry species would appear. However, for a trans-planar structure one would expect the $X(YX)Y$ experiment to contain a mixture of A_g and B_g species. Clearly, it is shown in Figure 3 that the $X(YX)Y$ spectrum contains, in addition to the intense A_g bands, a number of medium-to-strong bands not present in the $X(ZZ)Y$ spectrum and therefore attributable to the B_g species.

Additional support for a planar-zigzag conformation comes from an examination of the CH stretching region in both the IR and Raman spectrum. Hsu et al.[23] have used local symmetry arguments to show that the conformation of a CC bond can be determined by consideration of the spectral activity of the CH stretching vibrations in the IR and Raman spectrum. Which bands appear will be governed by the conformation of the CC bond connecting two $-CH_2-$ groups. If this bond is gauche, all four CH stretches would appear in both the IR and Raman spectra. In the case of a trans bond one asymmetric and one symmetric stretch should appear in the Raman while the other two, obeying the mutual exclusion rule (a local inversion center exists), will be observed in the IR but their frequencies will be different from those observed in the Raman. Our experimental results indicate that two Raman bands are observed at 2992 and 2966 cm^{-1} while those in the IR appear at 2975 and 2960 cm^{-1}. Thus these results suggest that the conformation of the CC bond joining the two $-CH_2-$ groups is trans. Again considering the 3/2-helical conformation it becomes apparent that a trans CC bond is incompatible with such a structure.

When all the spectroscopic data already presented are taken collectively, it appears that the alternating E–TFE copolymer crystallizes predominantly in an all-trans planar structure in the solid state.

D. Assignments. Based on a planar-zigzag structure with factor group C_{2h} the number of normal modes and the spectroscopic selection rules have been determined by Kobayashi et al.[18] The vibrations are distributed among the symmetry species as follows: 10 A_g (Raman active), 7 B_g (Raman active), 7 A_u (IR active), and 8 B_u (IR active). In addition, all overtones will be Raman-active A_g modes while combinations of an $A_g + B_g$ or an $A_u + B_u$ will have B_g character. As seen in Table I it is possible to choose directions of the incident and analyzed radiation that will only allow observation of A_g modes in the Raman spectrum. Consulting the $X(ZZ)Y$ spectrum of Figures 3 and 4 it is possible to definitely assign modes at 2966, 1441, 1299, 1037, and 835 cm^{-1} to the A_g symmetry species. Assignment of these A_g modes is supported by consulting the $X(ZX)Y$ spectra, in which the A_g modes are expected to exhibit diminished intensity. The assignment of the remaining five A_g modes cannot be done unambiguously simply by reference to Figure 3. For this reason, a second scattering geometry (no. 2), depicted in Figure 2, was chosen. For this geometry, calculation of the derived orientation-averaged polarizabilities, α_{FF}^2, according to eq 2 using a transformation matrix Φ, determined from the relationship between molecular and laboratory axes shown in Figure 2, gives

$$\alpha_{ZZ}^2 = \tfrac{3}{8}(\alpha_{yy}^2 + \tfrac{2}{3}\alpha_{yy}\alpha_{zz} + \alpha_{zz}^2) + \tfrac{1}{2}\alpha_{yz}^2 \qquad \text{(geometry 2)}$$

If this expression is compared with that obtained for the $X(YX)Y$ experiment in geometry 1 (Figure 1)

$$\alpha_{YX}^2 = \tfrac{1}{8}(\alpha_{yy} - \alpha_{zz})^2 + \tfrac{1}{2}\alpha_{yz}^2 \qquad \text{(geometry 1)}$$

only the last term, $^1/_2\alpha_{yz}^2$, contributes identically to the two spectra and is the sole contributor of intensity to the B_g modes in these two expressions. Hence, the corresponding Raman measurements should preserve the intensity of B_g modes while that of A_g modes, which depend on α_{yy} and α_{zz}, would be expected to change.

The results are shown in Figure 5, where both spectra have been normalized to the intensity of the 1153-cm^{-1} band, which is assigned to a B_g mode since it is absent in the $X(ZZ)Y$ spectrum (obtained in geometry 1), which

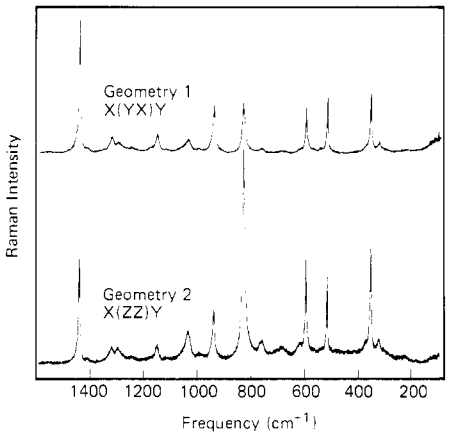

Figure 5. Raman spectra (100–1600 cm^{-1}) of E–TFE filament obtained from two scattering geometries. Spectra normalized to intensity of band at 1153 cm^{-1}.

Table III
Assignment of Additional Bands Observed in the Raman Spectra of E-TFE Copolymer

freq, cm^{-1}	assignment
2897, 2870	CH stretch in $(-CH_2CH_2-)_n$ with $n \geq 2$
1411	crystal field splitting of 1441 cm^{-1} $-CH_2-$ bending; overtone of an IR or Raman band
1057	CC stretch $(-CH_2CH_2-)_n$ $(n \geq 2)$
765[a]	CF stretch + CC stretch $(-CF_2CF_2-)_n$ $(n \geq 2)$
627[a]	CF_2 bending $(-CF_2CF_2-)_n$ $(n \geq 2)$
319	CF_2 rocking $(-CF_2CF_2-)_n$ $(n \geq 2)$ crystal field splitting of 328 (B_g)
16.5	longitudinal acoustical mode

[a] Observed in perfluorobutane.[25]

contains only A_g modes. By comparison, it becomes apparent that in addition to the A_g modes already identified, bands at 600, 520, 360, and 234 cm^{-1} exhibit A_g symmetry since they undergo intensity changes. Correspondingly, bands at 1321, 1153, 945, 328, and 132 cm^{-1} do not exhibit any intensity fluctuations and are therefore assigned to B_g modes. Remaining B_g modes can be assigned by comparison of the $X(ZZ)Y$ (geometry 1) and $X(ZX)Y$ spectra in Figures 3 and 4 since in the $X(ZX)Y$ spectrum, the A_g modes are expected to lose intensity. Thus, the 2992- and 1247-cm^{-1} bands belong to the B_g symmetry species.

Since only nine of the ten expected A_g modes can be assigned straightforwardly, the case of accidental degeneracy was considered. The band at 945 cm^{-1}, which has already been convincingly assigned, may in fact have a small A_g component as evidenced by Figure 3, where a band of weak-to-medium intensity is present in the top spectrum, in which only the totally symmetric modes should be observed. Thus, the 945-cm^{-1} band is also tentatively assigned to the A_g symmetry species.

In general, the assignments made above agree with those proposed by Kobayashi et al.[18] However, several of the polarized bands observed in this work differ from the experimental findings or the results of the normal coordinate calculations that were presented. This may reflect an inadequately refined force field and may require its reexamination upon consideration of these new assignments.

There are a number of additional weak bands that are observed in the Raman spectra and do exhibit polarization anisotropy. These are listed in Table III and generally can be assigned to short blocks of hydrocarbon[24] and/or fluorocarbon chains[25] which are contained in the backbone as defects. The band at 1411 cm^{-1} may be an exception since it may arise from crystal field splitting of the 1441-cm^{-1} $-CH_2-$ bending mode. This identical assignment[26] has been made for the 1411-cm^{-1} band observed in polyethylene and arises because of the packing of chains (2) into an orthorhombic unit cell. Likewise, information concerning the crystal structure of the E–TFE copolymer may be provided by a detailed study of crystal field splitting in the low-temperature infrared and Raman spectrum and further experiments have been undertaken.

An alternative assignment of this 1411-cm^{-1} band to an overtone of an IR or Raman fundamental is also possible. As discussed earlier all overtones will have A_g symmetry as is observed for the band at 1411 cm^{-1}.

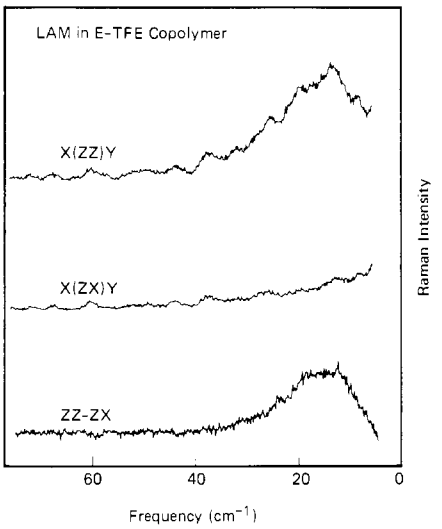

Figure 6. Polarized Raman spectra of the low-frequency LAM. Bottom trace has been corrected for stray light and I_2 contributions.

E. Observation of the Longitudinal Acoustical Mode (LAM). A very intense band located at 16.5 cm^{-1} (after correction for the effects of stray light, frequency, and temperature on the observed intensity[16]) was observed in both the Stokes and anti-Stokes Raman spectrum. As shown in Figure 6 this mode exhibits anisotropic scattering properties and appears in the $X(ZZ)Y$ spectrum while it is absent in the $X(ZX)Y$, $X(YZ)Y$, and $X(YX)Y$ spectra. The last two measurements are not included in Figure 6 since the scattering curves are identical with that of the $X(ZX)Y$ spectrum. This band belongs to the totally symmetric symmetry species and since no low-frequency modes are predicted[18] to lie in this region, the possibility that this intense band could be attributed to LAM was investigated.

Although it has been shown by Fanconi and Crissman[27] that the influence of a methyl group on the LAM frequency of a paraffinic chain is a function of its position along the backbone, with the maximum effect occurring when it is attached at the chain end, the existence of LAM in a chain with alternating chemical groups having significantly different masses has not been investigated. For this reason, normal coordinate calculations of such a model were undertaken. For this purpose, two different force fields (Table IV) were used, with both the $-CF_2-$ and $-CH_2-$ groups being approximated by point masses having values of 50 and 14 amu, respectively. A 38-atom planar-zigzag chain with alternating E and TFE units was constructed using CC bond lengths of 1.54 Å and CCC bond angles of 112°. The first set of valence force constants (set 1) was taken from the work of Shimanouchi and

Table IV
Force Constants[a] Used in the Calculation of LAM

	set 1	set 2
CC stretch, mdyn/Å	4.620	3.963
CCC bend, (mdyn·Å)/rad²	1.000	0.942
CC,CC stretch-stretch, mdyn/Å	0.132	0.148
CCC,CC bend-stretch, mdyn/rad	0.170	0.492
CCC,CCC bend-bend, (mdyn·Å)/rad²	0.300	0.166
CCCC torsion, (mdyn·Å)/rad²	0.087	0.149

[a] Set 1: force field for calculating LAM in paraffins using backbone approximation.[28] Set 2: force field for calculating normal modes of E-TFE copolymer.[18]

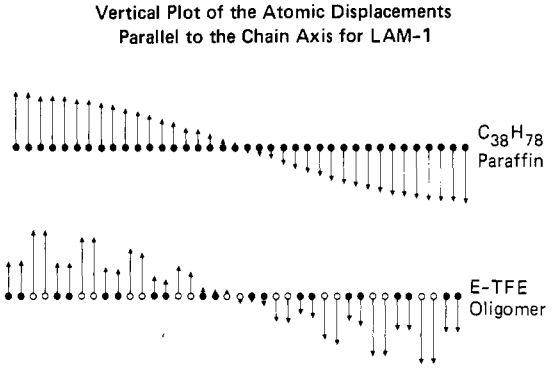

Figure 7. Vertical plot of the mass-weighted longitudinal Cartesian displacements for LAM-1 in $C_{38}H_{78}$ and an alternating E–TFE oligomer of the same length: open circles, $-CF_2-$; solid circles, $-CH_2-$.

Tasumi[28] since it was explicitly determined to calculate LAM in paraffins using the skeletal backbone approximation. In this case, the calculation of LAM was made by simply replacing the masses of alternating pairs of backbone atoms by that of $-CF_2-$ groups.

The second set of valence force constants was extracted from a larger set[18] used to calculate the normal modes of the infinite chain E–TFE copolymer. In this case, the set of alternating masses used was identical with that of the previous calculation. Interestingly enough, the choice of force field made little difference quantitatively or qualitatively on the result obtained for LAM in the E–TFE copolymer. In Figure 7 is shown a vertical plot of the longitudinal mass-weighted Cartesian displacements for LAM-1 in an alternating E–TFE oligomer and for a hydrocarbon chain of the same length. Since the backbone is trans planar, the dot product method of Reneker and Fanconi[29] was used in order to quantify the amount of longitudinal character present in the LAM-1 of the E–TFE oligomer. According to this criterion, a 38-component unit vector consisting of the normalized atomic displacements in the chain axis direction was formed for each molecule exhibiting a LAM vibration. A dot product was then formed between this vector for a pure hydrocarbon chain and a similar vector constructed for the alternating E–TFE oligomer. In the general case, this product has a magnitude between 0 and 1.0, indicative of the amount of longitudinal character present in this mode. A dot product value of 1.0 would indicate that the intensity of the mode would have a similar intensity to that of LAM-1 in a pure hydrocarbon chain. A value of 0.95 is obtained when this dot product method is applied to the E–TFE oligomer. Hence, these calculations indicate that a LAM does exist in the alternating copolymer and furthermore its intensity should be similar to that of its hydrocarbon analogue.

Calculated frequencies of 39.8 (set 1) and 40.3 (set 2) cm^{-1} were obtained for the 38-atom E–TFE oligomer compared to 58.4 cm^{-1} obtained for the corresponding $C_{38}H_{78}$ chain. Any attempt to use these values quantitatively would, at best, be speculative since the effect of using a skeletal backbone approximation to calculate LAM in an E–TFE copolymer has not been determined.

Based on the above calculations and the spectral behavior of the observed low-frequency mode, the 16.5-cm^{-1} band is assigned to the LAM-1 vibration of the E–TFE copolymer. It should be noted that although this band exhibits A_g symmetry it is not a normal mode of the infinite polymer chain but instead becomes Raman active because of a breakdown in the optical selection rules due to isolation of chain stems within a lamella by folds at the surface. Hence this band is not contained in the symmetry assignments for the infinite E–TFE chain in Table II.

It is also interesting to realize that, because of the accordion-like motion along the chain axis characteristic of LAM, the most significant contribution to the band intensity comes from the change in polarizability parallel to the chain axis, α_{xx}. Therefore, although A_g modes (Table I) are expected to appear in all four scattering geometries, only the $X(ZZ)Y$ spectrum contains modes whose intensity is proportional to α_{xx} and would thus be expected to contain LAM. Such is, in fact, the case.

As mentioned previously, SAXS photographs indicate that the copolymer lamellae have their normals oriented at an angle of 36–38° with the filament axis. A long period of 127 ± 10 Å was obtained for the E–TFE filament. Since it was concluded from Raman polarization measurements on LAM that the copolymer chains were also parallel to that filament axis, then they must also be inclined at an angle of 36–38° with respect to the lamellar normal. Thus, the traverse length across the copolymer lamellae at an inclination of 36–38° (with the lamellar normal) becomes 162 ± 10 Å. Considering that E–TFE copolymers have been reported[8] to have volume fraction crystallinities of 50–65% it is not unreasonable to expect that highly drawn extruded filaments would be somewhat higher. Conservatively taking a value of 70% for the crystallinity of the sample used in this study yields a value of the crystalline stem length of 113 ± 10 Å.

To put the observed LAM frequency of the E–TFE copolymer in perspective, a correspondence with LAM in slightly helical (2.14/1) PTFE can be made using the uniform elastic rod approximation.[30] It should be noted that the density of PTFE is 2.3 g/cm^3 while that for E–TFE is 1.91 g/cm^3 and hence any quantitative comparison of LAM in these two polymers must reflect the inverse relationship between the observed frequency and the density (ν is proportional to $\rho^{-1/2}$) as specified by the elastic rod model. A stem length of 113 ± 10 Å in PTFE[31] would give rise to a LAM-1 frequency of 13.3 cm^{-1}. The observed value of 16.5 cm^{-1} in E–TFE copolymers is slightly larger even when the density difference is taken into account. Thus, there is less flexibility in the E–TFE backbone (therefore, a higher LAM frequency), indicating that the conformational structure is more planar than a 2.14/1 helix and in all probability exists as a trans-planar structure.

It therefore appears that LAM is a very sensitive measure of conformation in the solid state and these measurements support our previous conclusions concerning the conformational structure of the E–TFE copolymer obtained from infrared and polarized Raman spectroscopy.

Conclusion

Polarized Raman measurements of the anisotropic scattering properties of a uniaxially oriented sample of E–TFE copolymer indicate that the conformation of the backbone is planar zigzag. This has been determined by comparing the Raman scattering results for four different

combinations of incident and scattered polarizations with those predicted by group theoretical analysis of an isolated chain in either a 3/2-helical or planar-zigzag conformation.

Observation of the Raman-active LAM and the correlation of its position with the corresponding stem length in lamellar crystals provide further evidence of a trans-planar structure.

Combined infrared and Raman measurements in the CH stretching region indicate, based on local symmetry arguments, that the CC bond joining the two CH_2 groups must be trans. Although this constitutes a necessary but not sufficient condition for planarity, when taken collectively with the additional results already described, it strongly supports the existence of a planar structure for the E–TFE copolymer in the solid state, as has been predicted by Farmer and Lando.[14]

Acknowledgment. We thank E. S. Clark (University of Tennessee) and T. Russell (IBM) for obtaining the WAXS and SAXS photographs of the E–TFE copolymer filament.

Registry No. E–TFE, 25038-71-5.

References and Notes

(1) Carter, V. B. *J. Mol. Spectrosc.* **1970**, *34*, 356.
(2) Bailey, R. T.; Hyde, A. J.; Kim, J. J. *Spectrochim. Acta, Part A* **1974**, *30A*, 91.
(3) Boerio, F. J.; Bailey, R. A. *J. Polym. Sci., Polym. Lett. Ed.* **1974**, *12*, 433.
(4) Bailey, R. T.; Hyde, A. J.; Kim, J. J.; McLeish, J. *Spectrochim. Acta, Part A* **1977**, *33A*, 1053.
(5) Rabolt, J. F.; Fanconi, B. *Macromolecules* **1978**, *11*, 740.
(6) Satija, S.; Wang, C. H. *J. Chem. Phys.* **1978**, *69*, 2739.
(7) Abenoza, M.; Armengaud, A. *Polymer* **1981**, *22*, 1341.
(8) Modena, M.; Garbuglio, C.; Ragazzini, M. *J. Polym. Sci., Polym. Lett. Ed.* **1972**, *10*, 153.
(9) Pireaux, J. J.; Riga, J.; Caudano, R.; Verbist, J.; Gobillon, Y.; Delhalle, J.; Delhalle, S.; Andre, J. M. *J. Polym. Sci., Part A-1* **1979**, *17*, 1175.
(10) English, A. D.; Garza, O. T. *Macromolecules* **1979**, *12*, 351.
(11) Clark, D. T.; Feast, W. J.; Ritchie, I.; Musgrave, W. K. R.; Modena, M.; Ragazzini, M. *J. Polym. Sci., Part A-1* **1974**, *12*, 1049.
(12) Garbuglio, C.; Modena, M.; Valera, M.; Ragazzini, M. *Eur. Polym. J.* **1974**, *10*, 91.
(13) Wilson, F. C.; Starkweather, H. W., Jr. *J. Polym. Sci., Part A-2* **1973**, *11*, 919.
(14) Farmer, B. L.; Lando, J. B. *J. Macromol. Sci., Phys.* **1975**, *B11*, 89.
(15) Devlin, G. E.; Davis, J. L.; Chase, L.; Geschwind, S. *Appl. Phys. Lett.* **1971**, *19*, 138.
(16) Snyder, R. G.; Scherer, J. R. *J. Polym. Sci., Part A-2* **1980**, *18*, 421.
(17) Billmeyer, F. W., Jr. In "Textbook of Polymer Science"; Wiley: New York, 1971.
(18) Kobayashi, M.; Tashiro, K.; Tadokoro, H. *Macromolecules* **1975**, *8*, 158.
(19) Alexander, L. E. In "X-Ray Diffraction Methods in Polymer Science"; Wiley-Interscience: New York, 1969.
(20) Damen, T. C.; Porto, S. P. S.; Tell, B. *Phys. Rev.* **1966**, *142*, 570.
(21) Snyder, R. G. *J. Mol. Spectrosc.* **1971**, *37*, 353.
(22) Schlotter, N. E.; Rabolt, J. F., to be published.
(23) Hsu, S. L.; Sibilia, J. P.; Obrien, K. P.; Snyder, R. G. *Macromolecules* **1978**, *11*, 990.
(24) Hendra, P. J.; Jobic, H. P.; Marsden, E. P.; Bloor, D. *Spectrochim. Acta, Part A* **1977**, *33A*, 445.
(25) Campos-Vallette, M.; Rey-Lafon, M. *J. Chem. Phys.*, in press.
(26) Strobl, G. R.; Hagedorn, W. *J. Polym. Sci., Part A-2* **1978**, *16*, 1181.
(27) Fanconi, B.; Crissman, J. *J. Polym. Sci., Polym. Lett. Ed.* **1975**, *13*, 421.
(28) Shimanouchi, T.; Tasumi, M. *Indian J. Pure Appl. Phys.* **1971**, *9*, 958.
(29) Reneker, D. H.; Fanconi, B. *J. Appl. Phys.* **1975**, *48*, 4144.
(30) Schaufele, R. F.; Shimanouchi, T. *J. Chem. Phys.* **1967**, *47*, 3605.
(31) Rabolt, J. F.; Fanconi, B. *Polymer* **1977**, *18*, 1258.

Effect of Polymer Chain Tacticity on the Fluorescence of Molecular Rotors

Rafik O. Loutfy*

Xerox Research Centre of Canada, 2480 Dunwin Drive, Mississauga, Ontario L5L 1J9, Canada

David M. Teegarden†

Webster Research Center, Xerox Corporation, Webster, New York 14580.
Received January 14, 1982

ABSTRACT: The fluorescence properties of julolidinemalononitrile (1), a molecular rotor probe, have been studied in a series of stereoregular poly(methyl methacrylate) films. The quantum yield of fluorescence of 1 was found to be dependent on the tacticity of the polymer. The relatively high fluorescence yield of 1 in isotactic PMMA indicated that the flexibility of isotactic chains is lower than that of syndiotactic or atactic PMMA. The temperature-dependent fluorescence results are consistent with a helical conformation for isotactic PMMA.

In recent years methods have become known for the preparation of high molecular weight stereoregular isotactic and syndiotactic poly(methyl methacrylate),[1] (*i*- and *s*-PMMA) (see Figure 1). These species exhibit vastly different properties from the so-called atactic (a-PMMA) or random polymers. Both the isotactic and syndiotactic PMMA polymers have been characterized through differences in X-ray diffraction patterns,[2] infrared spectra,[3] laser Raman spectra,[3] far-ultraviolet spectra,[4] densities,[5] glass transition temperature,[6] dielectric loss curves,[7] and mechanical and viscoelastic properties.[8] Information on the steric arrangements of functional groups is best provided by high-resolution NMR techniques.[9]

Although certain of these measurements have given direct information on the tacticity of these polymers, the

†Present address: Department of Chemistry, St. John Fisher College, Rochester, NY 14618.

0024-9297/83/2216-0452$01.50/0